Politecnico di Torino

The Zero Risk Society

A COVID application

Supervisor
Prof. Didier Sornette, ETH Zürich
PhD. Giuseppe Maria Ferro, ETH Zürich
Prof. Luca Dall'Asta, Politecnico di Torino

Author
Francesco Maria Russo

A Master Thesis presented for the Master Degree in

Physics of Complex Systems

Politecnico di Torino

ETH zürich

Politecnico di Torino
Université de Paris
Eidgenössische Technische Hochschule (ETH)

ACADEMIC YEAR 2020-2021

Introduction: The Zero Risk Society

Human society can be considered an out of equilibrium system characterised by a complex evolution often perturbed by extreme rare events. These perturbations can be both exogenous like pandemics or earthquakes and endogenous like financial crises, wars, scarcity of resources etc. Some of these stressors may also be real unknown unknowns and, therefore, impossible to predict. For this reason, a vital ingredient of a resilient society is not trying to prevent and control all the unpredictabilities that we may face. Indeed this rush towards eliminating all the risks and be assured against everything leaves society extremely vulnerable to the aforementioned calamities [1]. Instead, a healthy society aims to balance the natural and riskless incremental accumulation of knowledge with bold leaps of faith, leading to new revolutionary inventions that advance humanity forward. In other words, great challenges require the opportunity, empowerment, and the willingness to take risks to find solutions. Humanity, however, seems aimed in the opposite direction. Over the past decades, we have been experiencing stagnation mostly (but not also) in the fields of technology and economics by confusing revolutionary inventions with apps that have a marginal impact on our life and we have experienced a decline in new risky but visionary investments. Five leading causes are believed to be responsible for this frozen *"Zero Risk"* phase of society [2], and they are:

1. Risk aversion as a consequence of increasing wealth and aging of society;
2. Increasing inequality with a growing proportion of citizens that have no or less access to opportunity forced to live by the day;
3. Technology creating the illusion that everything can be controlled;
4. Herding and imitation behaviour of the population through social media;
5. Management shaped by extremes and overreaction.

This work is part of a bigger project in observing the Zero Risk *phase transition* of society we described above by creating an agent-based model in which the individuals are embedded in a society with the previously mentioned characteristics.

One effort that I will call I Zero Risk Society, described in the thesis project of my colleague Aventaggiato, tackles more directly the issue of the lack of investment in risky, and possibly revolutionary, assets characterised by this phase of society. The perturbation is in this case the high volatility of the risky asset the agents may want to invest in.

The present work, on the other hand, aims to contextualise the original project of the Zero Risk Society in a particular scenario when an exogenous stressor like a

pandemic along the lines of COVID19 hits society in order to show how the causes that led to the paralysation of the society have the same effects no matter the type of perturbation.

Acknowledgements

First and foremost, I would like to thank my supervisor, professor Didier Sornette for giving me the opportunity to participate in the first of many steps of this inspiring project. Besides achieving my MSc thesis goal, I found myself firmly aligned with the premises this work is built on. These lessons that I find of critical importance for shaping a better future for society will surely guide my very own future decision-making.

Many thanks are also owed to my supervisor PhD Giuseppe Ferro, who guided the thesis's development in a light-hearted and ironic fashion, especially during the surprisingly prolific meetings in the kitchen of the risk-advisory building where most of the ideas were developed.

None of what I achieved would have been possible without my parents and brother's ever-present support. You have always guided me and spared me of any worry, and you will always be my model on how to be a righteous and reliable person. I owe everything to you.

As part of my family, I also thank my fiancé Caterina. You always drew the lightest, brightest and most positive side of me but also took care of the most grumpy and blithesome bits. You made the time spent in quarantine a time worthwhile remembering for good as all the time I have spent with you.

I was also blessed with the most witty, unique yet responsible group of friends: Fulvio the charmer, Luca the CEO, Cristina the clockwork, Marta the dormouse and Giada the Pythia. Countless the time and the experiences we share, as are the thanks I owe you. I am sincerely delighted to see your early careers unfold, and I will always hope for the best to happen to all of you.

A final thanks to my coworker and friend Giuseppe, who helped me during the thesis development for sure, but especially through the most bitter and PTSD-inducing experiences during the years of the Master.

Thanks to the crew of Sihlweidstrasse for giving Giuseppe and me a warm and friendly welcome in Zurich during the final step of our academic path.

Contents

List of Tables

List of Figures

1 Overview of the model

In order to describe the social phase transition induced by the ingredients presented previously in the context of a pandemic, we devised a multiplex network approach with two coupled stochastic processes, one on each of the networks. The first process describes the "social contagion": the spreading of information and fear in the *social media network* reinforced and amplified by the herding behavior of the individuals and the sensationalist and distorted news reported by the media. On the other hand, the second one describes the spreading of the disease across the "real-life" network. The main papers that inspired this idea of a multiplex network are the ones of Fast et al. [5] and da Silva et al. [6] that we appropriately modified to suit our needs. In particular, the work of Fast et al. is able to correctly reproduce the different social responses that a disease (as for the SARS outbreak in Honk Kong in 2003 or H1N1 influence in Hong Kong and Mexico in 2009) can induce in a population based on its perceived risk, and not only on its objective lethality or persistence in the population. Moreover, their work highlighted the importance of the coupling between the health state of individuals during the epidemic (therefore the spreading of the disease) and the spread of information or fear on the disease itself not only perpetrated by the individuals but also coming from an external media to which all agents are subjected. This last external contribution, in particular, is fundamental in increasing the social anxiety in the population during the spreading of a disease, in the cases where the objective persistence in the population is very low, and there are no "personal" or direct relations with sane and infected individuals in the population. However, their model lacks the reverse coupling: how the social response due to the spreading of a disease influences the course of the epidemic itself that will then change the social response again in return and so on. On the other hand, the work performed by Da Silva et al. considers this last aspect but lacks the contribution of an external source of information (the media) that in the modernized world has become a pervasive force able to influence society significantly. This type of modelling feels natural to us to capture the behaviour (in our case study the risk propensity) of individuals in response to perturbations coming from the outside world they contribute shaping with their very own behaviour. Indeed, in our model, we will see how the information spreading across the social network about the epidemic, by changing people's behaviour, will inevitably influence the spreading of the epidemic itself in the real network. At the same time, the change course of the epidemic due to people awareness will unavoidably change the spreading of ideas/fear in the social network. We will proceed now in describing one by one the key elements of our model.

2 Age distribution and health capital

As stated in the introduction, one of the main cause that we believe leads towards the Zero Risk Society is the progressively aging and therefore increasing risk aversion of the population. In order to account for this factor we extracted the age A of each individual in the population in our model from the real data of age population distribution coming from [7]. We sampled the agents' age starting from $15 \div 19$ until 100+ age to take into account only the portion of the population that acts "consciously". Afterwards we normalized this range from 0 to 1. We then converted the age in what we will call the *health capital* Θ: a quantity representing the amount of resilience of an individual to a disease and that therefore will influence his risk propension (see section 4.2). Following the intuition that generally a youth will be more resilient than an elder we simply defined the health capital of agent i as:

$$\Theta_i := 1 - \mathrm{A}_i. \tag{2.0.1}$$

Two of the age distributions that we sampled can be found in Fig.(1) For now we notice without much surprise how, especially in a modernized society (like Italy), the population got older and older; we will see in the following sections where we describe our model in full details how these differences will fit in.

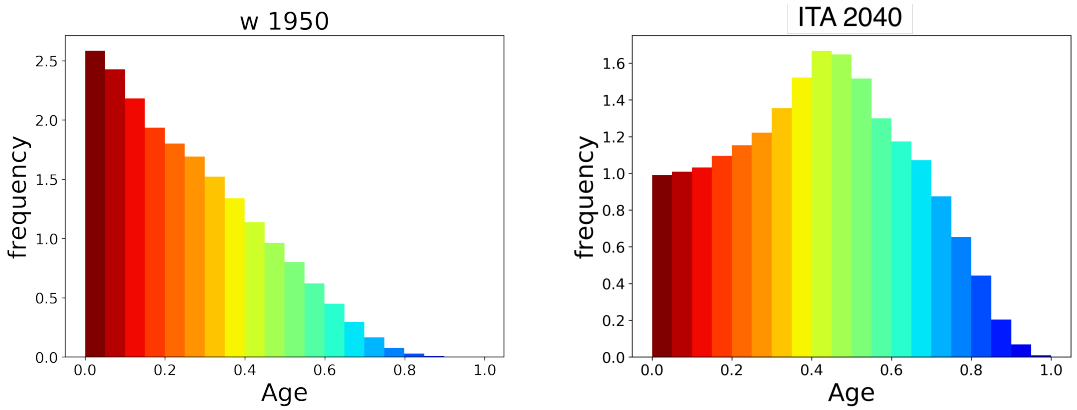

Figure 1: Left: age distribution in the world in 1950. Right: forecast of the age distribution in Italy in 2040.

3 Networks topology

3.1 A brief introduction to networks

The role of networks is crucial in every field that deals with complex systems characterised by the interactions of multiple agents: ranging from statistical mechanics and spins systems, neuroscience, computer science and sociology [8]. A network, in mathematical terms, is described by a *graph*. A graph G is an ordered pair $G = (V, E)$ where V is called the set of vertices (or nodes) and $E \subseteq V \times V$ is called the set of edges: the elements of the graph that join the vertices together. The number of edges connected to a node is called its *degree* k and with the notation ∂i we will indicate the nearest neighbours of node i. Graphs are usually represented graphically as a collection of dots, each corresponding to a node; a line then joins two dots if the corresponding nodes are connected by an edge. A *path* in a graph G is an ordered sequence of vertices $p = (v_0, \dots, v_n)$ all belonging to V such that $(v_i, v_{i+1}) \in E$, and its length is defined as $|p| = n$.

3.1.1 Random graphs

Traditionally, systems with a complex topology beyond a regular lattice have been described using two very famous types of random graphs: the Erdős–Rényi (ER) $G(N, n)$ or $G(N, p)$ random graph or the Watts-Strogatz (WS) Small World network [9]. The $G(N, n)$ random graph with N number of nodes and n number of edges, as introduced in the original paper [10], is built by randomly choosing the n edges in the graph among the $\binom{N}{2}$ total possible ones. In this way, we extract a graph with uniform probability among the $\binom{\binom{N}{2}}{n}$ graphs with N nodes and n number of edges decided a priori. On the other hand, in the $G(n, p)$ model, we avoid fixing the number of edges a priori and assign a probability p of "existing" in the final graph to each edge instead. Therefore, the total number of edges in the network $|E|$ will be this time a binomial random variable with mean $\binom{N}{2}p$. Clearly, in the limit of large N, a $G(N, p)$ graph will almost surely have a number of edges equal to the average value by the law of large numbers. Consequently, a $G(N, p)$ random graph should behave similarly to a $G(N, n)$ with $n = \binom{N}{2}p$. Similarly to the total number of edges, in the $G(N, p)$ graph also the degree k of a node will be distributed according to a binomial distribution with probability:

$$P(k) = \binom{N-1}{k} p^k (1-p)^{(N-1)-k} \tag{3.1.1}$$

since a node can be connected at most with the remaining $N-1$ nodes in the network, giving rise to the typical bell shape distribution of the nodes degree in the network. Thus, the resulting system will be deeply democratic despite the random placement

of the edges, and most nodes will have approximately the same number of links close to the average value. Random networks are also called exponential because the probability that a node is connected to k other sites decreases exponentially for k much greater than the typical value. As described in the original paper by Watts and Strogatz [11], small world networks are usually built starting from a regular lattice and rewiring each edge in the graph with a probability parameter $0 < p < 1$. Thus, a $p = 0$ will leave the graph unchanged, while for a $p = 1$, we will obtain a complete random graph. The most notable property of this kind of network is that for an intermediate value of p, the resulting graph shows a significant drop of the characteristic path length, defined as the number of edges in the shortest path between two vertices averaged over all pairs of vertices, typical of a random graph. However, the resulting graph will also retain the overall high density of neighbours each node has, typical of a regular graph. This generates the so-called small world phenomenon in which every node in the network is reachable from any other node through a short path composed of a small number of vertices. Both ER and WS networks possess very interesting properties intensively studied that we will not mention here for conciseness but can be found in [12][11][13]. For our purposes, it is sufficient to notice how the previous models, however, lack two crucial aspects that nevertheless define most real-life networks [9]: *growth* and *preferential attachment*.

3.1.2 Scale-free networks

Both the ER and WS graphs are built starting from the presence of N total nodes in the network altogether and, loosely speaking, by connecting them with a uniform random probability. Unlike ER and WS networks, most real-world networks were not created out of the blue with all the vertices in position but started with a handful of nodes and then *grew over time* by the continuous addition of new vertices to the system. In addition, the just added nodes in the network will not form an edge randomly with uniform probability with one of the pre-existing nodes of the network but will *connect preferentially* to a node with a large number of neighbours: the so-called "rich-get-rich" or alternatively "first mover wins" phenomena [9]. Growth and preferential attachment, at the foundation of the Albert-Barabási (AB) algorithm, play an essential role in lots of real network development and lead to the famous scale-free type of network characterised by the renowned power-law distribution of nodes' degree inside the network $P(k) \sim k^{-\gamma}$. As a consequence, in contrast to the democratic distribution of links seen in random networks, power laws describe systems in which a few nodes, called *hubs*, possess most of the links in the network.

Albert-Barabási algorithm: Start with a number of n randomly connected nodes, $n \ll N$, with N the number of final nodes in my system. At each step of the algorithm add a new node i to the network provided with m links. Attach the m links to an already present nodes j in the network with a probability:

$$\Pi(j) = \frac{k_j}{\sum_l k_l} \tag{3.1.2}$$

In particular, according to this algorithm, the rate at which the degree of node i increases (considering it a continuous variable) is:

$$\frac{\partial k_i}{\partial t} = m\Pi\left(k_i\right) = m\frac{k_i}{\sum_{j=1}^{N-1} k_j} \tag{3.1.3}$$

which results in a time evolution of the degree equal to

$$k_i(t) = m\left(\frac{t}{t_i}\right)^{\frac{1}{2}} \tag{3.1.4}$$

where t_i is the time at which node i was created in the network. This finally leads to the aforementioned power law nodes degree distribution

$$P(k) = \frac{2m^2}{k^3} \tag{3.1.5}$$

where the exponent $\gamma = 3$ is independent on the parameter m. As shown in [13][14][15], many real-world networks exhibit this type of degree distribution from the WWW and social networks to the citation patterns of the scientific publications and much more.

3.1.3 The Bianconi Barabási Model

The so-called Fitness model proposed by Bianconi e Barabási (BB) [16] gives a further enhancement of the previously discussed theory. It builds directly on the foundation given by the AB model by inserting a third essential ingredient: competitiveness of nodes in acquiring new links. In social systems, not everybody makes friends at the same rate. On the WWW, some web pages acquire many links quickly. Likewise, some research papers shortly acquire many citations due to the importance of their findings. This intrinsic ability of different nodes to acquire new links at different rate beyond their already established presence in the network is modelled in

the BB network using the *fitness* parameter η_j associated with node j. This change is inserted in the original AB algorithm by updating (3.1.2) as:

$$\Pi_F(j) = \frac{\eta_j k_j}{\sum_l \eta_l k_l}. \tag{3.1.6}$$

This slight modification in the algorithm allows for a much richer behaviour in the evolution of the fitness type network. Indeed the time evolution of k_i follows a power-law in time, but this time there is multiscaling in the system (the dynamic exponent β that characterises the growth of the node's i degree depends on the fitness η_i):

$$k_{\eta_i}(t, t_0) = m\left(\frac{t}{t_0}\right)^{\beta(\eta_i)}, \tag{3.1.7}$$

where t_0 is the time at which node i entered the network. Moreover the degree distribution in the network results in a weighted "sum" of power laws [16]:

$$P(k) \propto \int d\eta \rho(\eta) \frac{C}{\eta} \left(\frac{m}{k}\right)^{\frac{C}{\eta}+1}, \tag{3.1.8}$$

(where C is a costant) which depends on the whole distribution of fitness across the network $\rho(\eta)$. As a conclusive note, we cannot exempt ourselves from mentioning one remarkable connection between the evolution of fitness networks and a famous physical phenomenon: Bose-Einstein condensation. Loosely speaking, if a network grows according to the BB algorithms, in large times the evolving network will typically be in the "fit-get-rich" phase. Indeed, as opposed to the rich-get-rich phenomena, in the BB algorithms, the nodes that will acquire the majority of links in the network evolution will not necessarily be the ones that were present in the network from the beginning but will be the ones which have the greater fitness and successfully attract the majority of links during the growth and development of the network. Despite the presence of these hubs that dominate the network in terms of the number of connections, in this phase, even the fittest node's share of links decreases to zero for large times. However, some distributions of the fitness in the network lead to the so called "winner takes all" phase where in the competition for new edges the node with the largest fitness emerges as a clear winner. Despite the continuous emergence of new nodes that compete for links, it consistently earns a finite fraction of the edges. This phenomenon, through clever mapping, can be reduced to a BE condensation in an equilibrium Bose gas where, in the thermodynamical limit, the lowest energy level houses a finite share of the total number of particles in the system. For the sake of conciseness we will not mention here any results but we reference the original paper along interesting applications regarding the emergence of statistical outliers and dragon kings [17] in networks that cannot be interpreted with the aid alone of a power law distribution [18][19][20]. In the

subsequent section, we will analyse the type of networks we decided to implement in our model.

3.2 Social media network

As presented in the previous section, many social networks and even the WWW are comfortably described using a scale-free network. Moreover in the modern era, much human interaction takes place on the internet and social media. On these digital plazas, most of us are not only linked to relatives and friends we personally know but are also subjected to the influence of famous individuals we do not know directly yet are followed by the majority of the people in the network and therefore exercise much influence on our beliefs. For this reason, we decided to implement a scale free network for the social network where the spread of information among agents will take place, using the well known BA preferential attachment algorithm without the insertion of a fitness distribution across the nodes. An example of the network we obtained with the corresponding nodes' degree distribution can be found in Figs.(2,3). The network nodes will represent our agents, while the edges will represent the connection between them, thanks to which they can exchange information. The presence of hubs in our network will model the presence of very influential/popular individuals in the system who are more likely to influence others rather than be influenced. After the creation of the network, we associated each node with its health capital Θ and without any information on the dependence between "popularity" (that is, the degree of the node) and age, we considered them to be independent that is $P(\Theta_i|k_i) = P(\Theta_i)$. After the construction of the network, to take into account the herding and imitation behaviour that we believe plays a crucial role in advancing towards the Zero Risk Society, we went through all the edges in the network and preserved them one by one with a certain probability that we will call *Social Media Connectivity* (SMC). An SMC=1 will leave the network intact with maximum social connectivity, modelling a society similar to the one we are living in today. An SMC=0, resembling a civilisation in which social media have yet to pervade society, will remove all the edges in the network, thus eliminating the imitation behaviour from our model.

3.3 Disease spreading network

The network used to characterise the disease spreading in our model was inspired mainly by the work of Davis et al. and Vespignani et al.[21][4]. In both models, the authors analyse the spreading of a disease (or information) in a *Metapopulation network*. The metapopulation network is characterised at first by a "substrate" network of communities (subpopulations) inside which our agents live. It is easy to think about these communities, for examples, as cities. Inside each subpopulation, agents

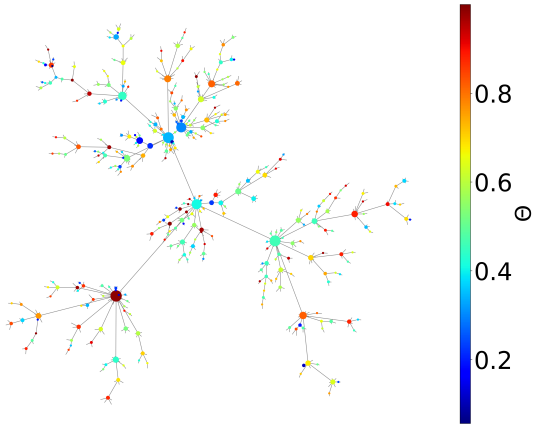

Figure 2: Example of the social media network in our model with $N = 1000$ spins, $m = 1$, $SMC = 1$ and age extracted from ITA 2040. The colorscale indicates the health capital Θ of the node while the size of the node is proportional to its degree.

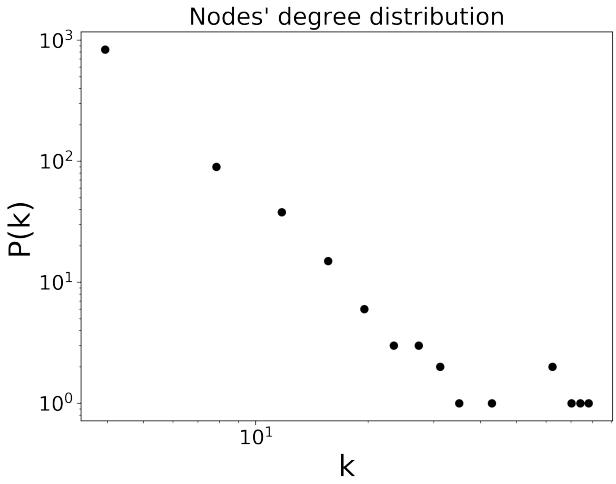

Figure 3: Degree distribution of the scale free network displayed on the left.

can interact, and if two communities are joined together by an edge, individuals can travel from a community to another. Therefore the number of agents inside a community, that is, its *size* $\mathcal{S}_i(t)$ can vary over time. The metapopulation network was built using the BB fitness model in which the fitness η of each subpopulation was extracted from a fat tail distribution $\rho(\eta) \sim \eta^{-\gamma}$ with $\gamma = 2.2$, as done in the cited paper by Davis et al. The fitness of each community extracted from the distribution will then become also the initial size $\mathcal{S}_i(t = 0)$ of the community itself, that is, the number of agents that at the beginning of the disease spreading will live there. In this way, in the construction of the network using (3.1.8), bigger cities will be also more connected. Inside each city i then, for simplicity, we organised the agents in a $G(S_i(t), p_i)$ network where we fixed $p_i = \frac{4}{S_i(t)-1}$ so each individual will be connected, on average, with four other agents inside the city. Example of these two networks can be found in Figs.(4,5). After describing the networks on which our stochastic processes will occur, it is now time to describe them in full detail. In the following section, we start by describing the model for the information spreading in the social network.

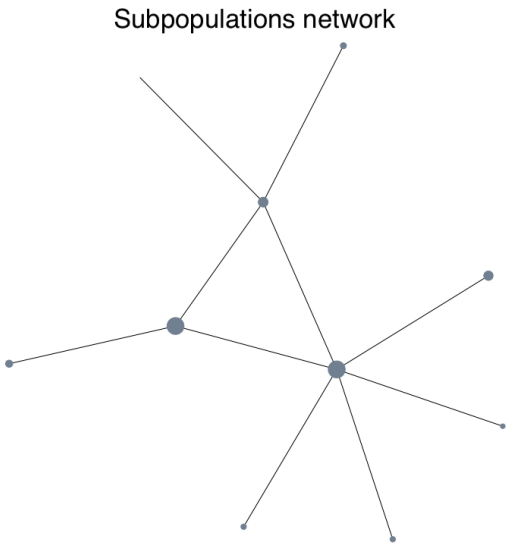

Figure 4: Subpopulations network of cities built using the BB fitness model.

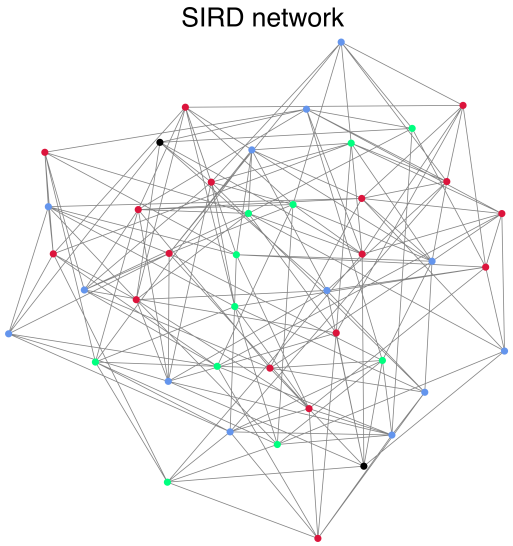

Figure 5: Example of the network of agents inside each community. The colors of the nodes label the different state of each individual in the SIRD model. More details will be given in the SIRD section.

4 Information spreading model

4.1 A brief review on opinion dynamic models

In the last decades, there have been growing interests in applying the models and tools developed in complex systems to investigate various complex social phenomena. One significant subfield of this new research field is the so-called "opinion dynamics", which can be described as the research field in which mathematical and physical models are employed to explore the diffusion dynamics and the evolution of opinions in the human population. In recent years, the studies on opinion dynamics models have attracted wide attention, especially in the statistical physics community, since most of the models used in this new field of research draw much inspiration from already existing models and methods utilised in statistical physics. As stated before, opinion dynamics models study the process of individual opinion evolution. The interactive agents in the population constantly update their opinions on a given issue based on specific evolution rules of the models until they reach a stable phase at the final stage, forming a consensus, polarisation, or fragmentation opinion distribution. A complete review of these types of models can be found in [22][23]; here, we will only give a general flavour regarding the most popular ones. Indeed most of these

models share a lot in common: most of them are agent-based models where the dynamics of opinions are determined by the local rules of inter-agent interactions and by the topology of the network where the inter-agent interactions occur, and the opinions evolve.

4.1.1 The Voter model

The standard Voter model [24] is a discrete opinion dynamics model with all agents placed on a two-dimensional lattice. The opinion of each agent is encoded in the binary variable $\sigma_i \in \{+1, -1\}$. At each time step, an individual adopts the sign of the majority of the spins in its neighbourhood with a probability $1 - q$ and the minority sign with a probability q. In formulas:

$$w(\sigma_i) = \frac{1}{2}\left[1 - (1 - 2q)\,\mathrm{sign}(\sigma_i)\,\mathrm{sign}\left(\sum_{j\in\partial i}\sigma_j\right)\right]. \tag{4.1.1}$$

The probability q is the noise parameter of the model and acts as a "social temperature". A big value of q, in fact, promotes the formation of opposite pairs of opinion in the network. Several authors have studied this system and have shown how it undergoes a second-order phase transition when the critical noise reaches $q_c \approx 0.075$ and has the same universality class as the equilibrium two-dimensional Ising model. Majority-vote dynamics were also studied in several complex networks: small-world networks, random graphs, and scale-free networks[25]. However, many of these expanded and modified versions of the majority vote do not belong to the same universality class as the corresponding Ising model, while some present critical exponents that are indeed Ising-like. This supports the conjecture by Grinstein et al.[26] that states how irreversible systems with up-down symmetry belong in the universality class of the equilibrium Ising model only for regular square lattices. There have been many experimentations on the voter model also beyond changing the underlying network where the interactions occur. We will mention here two of them that were fundamental in shaping the built of our model of social interaction. The first variation was performed by Vilela and Stanley [25] to study the effect of more influential individuals in the network. Basically, a fraction of the population posses a value of the spin $|\mu_i| = 1.5$ greater than the $|\sigma_i| = 1$ of the average individual. However, it has to be noticed that despite having a significant influence over other agents, the strong opinion nodes in this model do not show any extra resistance in changing their own opinion and are influenced by others as anybody else in the network. In the second variation [27], Avella et al. included the contribution of the media opinion in the network. Briefly, the media is connected to each agent in the community and has an opinion equal to the one of the majority of the population. At each step of the evolution of the opinions in the network, each agent with a tunable probability may decide to connect with the media instead of

following the opinions of his neighbours. We will not discuss the authors' findings of both models; instead, we refer to the original papers for a more detailed analysis.

4.1.2 The Ising model

Another important opinion dynamic model very similar to the previous one is the well-known Ising model [22][23], originally used in physics to explain the phase transition of ferromagnetic materials [28]. The energy E of interaction between two magnetic dipoles in Ising's original work corresponds here to the degree of conflict of opinions between two agents, as shown below:

$$E = -h_i s_i - h_j s_j - J_{ij} s_i s_j. \tag{4.1.2}$$

In opinion dynamics, $s_i \in \{+1, -1\}$ indicates the binary opinion of agent i, and J_{ij} represents the interaction strengths among agents. The fields h may account for external information or personal preference possessed by the agents. The model is very similar to the Voter model, the only difference being the dynamic of opinions evolution in Ising that, considering 0 temperature, is performed by minimising the Hamiltonian function of the system:

$$H(\{s\}) = -\sum_{\langle ij \rangle} J_{ij} s_i s_j - \sum_j h_j s_j; \tag{4.1.3}$$

the notation $\langle ij \rangle$ indicates that sites i and j are nearest neighbors. The Ising model is also famous for exhibiting phase transitions not only in its standard equilibrium representation with deterministic couplings and fields but also in its kinetic variations with randomly varying in time and space field as described in [29][30][31]. Both of these models are generalisable to a continuous opinion variable, but having a more robust familiarity in working within a physical framework, we opted in the end for an XY model.

4.2 XY information spreading model

In order to describe the social phase transition towards the Zero Risk Society, we built an XY model (constrained in the first quarter, with all spins having an angle between 0 and $\frac{\pi}{2}$) of N interacting agents with quenched random fields varying in time and space. In this framework, an agent's opinion, and more specifically, risk propensity, can be encoded in the 2-dimensional spin variable $\mathbf{s}_i = (cos(\theta_i), sin(\theta_i))$, where θ_i describes the individual i risk propensity in the following term:

$$\theta_i = \frac{\pi}{2}(1 - P_i(\text{Exit})). \tag{4.2.1}$$

The risk propensity $P_i(\text{Exit})$ has to be interpreted in this model loosely as the individual's propensity to live his "normal" life during the epidemic's development

instead of confining himself inside his habitation for fear of contracting the disease. In this way, a spin laying flat on the x axis will represent a full risk taker willing to living his life no matter what for leisure or work, while a spin aligned on the y axis will represent a fully reclused individual. The order parameter of our model will naturally be the average exit probability across all agents, that is:

$$P_{\mathrm{E}} = \frac{1}{N}\sum_{i=1}^{N} P_i(\mathrm{Exit}), \tag{4.2.2}$$

that we will use to monitor the overall fear circulating in the population about the disease that is perturbing the normal course of their life.
The Hamiltonian of our XY opinion dynamic model is the following:

$$H(\{\mathbf{s}\}, t) = -\sum_{i=1}^{N}(\mathbf{h}_i(t) + \mathbf{h}_{\mathrm{m},i}(t)) \cdot \mathbf{s}_i - \frac{1}{2}\sum_{i=1}^{N}\sum_{j\in\partial i} J_{ij}\mathbf{s}_i \cdot \mathbf{s}_j. \tag{4.2.3}$$

We will now analyse each term singularly dropping the time dependence when not explicitly needed.

4.2.1 Idiosyncratic field

In our model, the idiosyncratic fields $\{\mathbf{h}_i\}$ represent the individual's personal "opinion" in taking risks without having interacted with other agents in the social network and are taken to be:

$$\mathbf{h}_i = |\mathbf{h}_i|(cos(\theta_i^*), sin(\theta_i^*)), \tag{4.2.4}$$

where θ_i^* represents the individual risk propensity of the agent, that is, without interacting with other individuals:

$$\theta_i^* = \frac{\pi}{2}(1 - P_i(\mathrm{Exit}^*|\Theta_i, X_i)), \tag{4.2.5}$$

$$P_i(\mathrm{Exit}^*|\Theta_i, X_i) = \Theta_i f(X_i), \quad X_i \in \{S, I, R, D\}, \tag{4.2.6}$$

$$f(X_i) = \begin{cases} 1 & X_i = S, R \\ \frac{1}{2} & X_i = I \\ 0 & X_i = D \end{cases}. \tag{4.2.7}$$

From the previous equations we can see how the probability of exit of individual i will depend both on his health capital Θ_i and his status X_i in the metapopulation network that will follow a SIRD epidemic spreading dynamics, that will be better described in its own section (5). In this way, young, "healthier" (high Θ) and sane ($X_i = S, R$) individuals will be more likely to go out (have a higher risk propensity), while an older and more fragile individual will be more cautious in taking chances.

On the other hand, regardless of the health capital, an infected individual ($X_i = I$) in the population will reduce his individual risk propensity by half because of emerging symptoms or personal awareness of carrying the disease. For a deceased individual moreover ($X_i = D$) $P_i(\text{Exit}^*|\Theta_i, X_i) = 0$. The modulus of the field is built as:

$$|\mathbf{h}_i| = \Theta_i k_i, \tag{4.2.8}$$

accounting for the fact that younger (higher Θ) or more influential individuals (higher k) in the network will be less likely to be influenced by other people and stick to their personal preference. The individuals' "opinion exchange" and subsequent influence among each other will be modeled by letting the spins thermalize using a Monte Carlo Markov Chain (MCMC) dynamic. This will allow each individual to change his risk attitude $\theta^* \to \theta$ after having undergone the "social pressure" of his neighbours and the big influencers in the network.

4.2.2 Couplings

The couplings in the Hamiltonian describe the strength of the interaction between two individuals: how much they influence each other and, consequently, change their individual risk propensity from θ^* to θ once they are subjected to their neighbour's pressure. Balancing the modulus of the coupling was not a simple task in this model, given that the agents are embedded in a scale-free social network as described in the network section (3.2) which possesses a high heterogeneity in the distribution of the degree across the network. Indeed, hubs in the social media network would easily unbalance the interaction either for themselves that have a high degree and are therefore subjected to the influences of lots of other individuals or for the less popular agents connected to them and subjected to their huge influence. To prevent this from happening, we set the couplings value to be:

$$J_{ij} = (\Theta_i||\Theta_j)(k_i||k_j), \tag{4.2.9}$$

where $||$ denotes half of the harmonic mean (as done between two resistors in circuit theory) between two quantities:

$$x||y \ := \frac{xy}{x+y}. \tag{4.2.10}$$

The key property of the parallel that helps us perfectly balancing the interactions is that $x||y < \min(x, y)$. To see that this work let us consider an example in which i is a hub and j a normal node and consider $|\mathbf{h}_i| = k_i$, $|\mathbf{h}_j| = k_j$ and $J_{ij} = k_i||k_j$ for simplicity. Since $k_j \ll k_i$ the coupling among the two nodes will be $J_{ij} \sim k_j$. This means that node j will be strongly influenced by node i by an amount comparable by his own "opinion" $|\mathbf{h}_j|$ without however being completely dominated. Moreover the

hub i will feel only a little influence coming from node j as it should be. However a huge number of "less important" individuals like j may eventually change his opinion as well. Reverting to the full problem, we balanced both the "popularity" share of the field modulus and the health capital side by multiplying both terms separately balanced together.

4.2.3 Media field

As stated in the introduction, the role of the media plays a significant role in transitioning toward a Zero Risk Society by mainly spreading and exaggerating bad news especially in the aftermath of a crisis or a disaster [32][33]. Indeed humans have a propensity to give more weight and react more strongly to negative news rather than positive ones. This negative bias in news selection then influence news production towards more sensationalists and less reliable scoops which is summarised by the journalistic motto "if it bleeds, it leads"[34]. During the disease spreading, the main "news" that will be available to the media and that will communicate to other agents in the network will be the number of deaths caused by the disease and the number of infected in the network, both parameters that can assess the disease severity and persistence in the population. The modulus of the media field at time t is built in two steps. First, we consider all the deceased individual in the network in the last iteration of the disease spreading with their health capital, that is: $\{\Theta_i^D\}$. The superscript D identifies that the health capital is the one of a dead individual. Then we do the same with the infected individuals but this time we multiply their health capital by the age dependent probability of dying after being infected $p_{ID}(\Theta)$ (more details about these mechanisms will be given in the disease spreading section), that is: $\{\Theta_i^I \,:\, \Theta_i^I = \Theta_i p_{ID}(\Theta_i)\}$. This account for the fact that healthy individuals will most probably not display symptoms of the disease and therefore will not make literally the news in the system, and, in general, that the amount of worries caused by the news about an infection in the population will be given by the probability that the infection will result in a future death. These two quantities are then considered altogether in descending order in $\Theta^x,\ x \in \{D, I\}$ that is: $\Theta_1^x > \Theta_2^x > \Theta_2^x > \dots$ and then combined in:

$$v(t) = \sum_{i=1}^{\Gamma} \frac{\Theta_i^x}{\Gamma}. \tag{4.2.11}$$

The parameter Γ will be another key parameter of our model that accounts for the mentioned *management by extremes*. When close to one, it describes the media propensity to amplify the worst possible news occurred in the system that in our model is embodied by the death of a very healthy individual in the population due to the spread of the disease. On the other hand, a large Γ model a media that averages the shocking news of the death of a healthy individual with the more common news of unhealthy peoples deaths, thus not focusing solely on the extreme rares event

that may happen in the system but giving a more fair picture of what is happening instead. Secondly, the media report news based on what happened in the previous W days. The way we can account for this is:

$$V(t) = \sum_{k=0}^{W-1} v(t-k)\beta^k, \quad 0 \leq \beta \leq 1, \tag{4.2.12}$$

where β is a discount factor that takes into consideration how older news will gradually be set aside in favour of more recent shocking ones. In the end, we take the media fields to be:

$$\mathbf{h}_{m,i}(t) = [(V(t)||\Theta_i)(N||k_i)]\hat{u}_y, \tag{4.2.13}$$

the direction being along the y axis since the media pushes individuals towards fear and therefore not risking, N is the number of agents in the system. As before, the first term accounts for the popularity share of the idiosyncratic fields modulus, considering the media as an agent connected to all nodes in the network. The second term considers that people of different age and, therefore, different susceptibility to the disease will be influenced by different types of news. We can see how when Γ is high, it will not reach the younger and healthier side of the population that will not perceive the disease as a threat to their health since averaging over many deaths will yield a V smaller than one, and the media field will be negligible with respect to young people's field. On the other hand, a small Γ may transmit the (extremely rare) news of a healthy individual's death with a health capital, and therefore a V, close to one comparable to the health capital of younger agents. This time, the media field will be comparable to even the younger agents ones, and therefore, media will influence their exit probability more effectively by pushing relentlessly and unfairly the message that even younger deaths are possible with a great probability.

5 Epidemic modelling

The topic of epidemic modelling is a huge one. There are many possible types of models from stochastic to deterministic, including simple or more elaborate topology, which categorise individuals in the population in different ways. This section will give an essential review and state the results of the principal types of ways in which an epidemic can be modelled. A more comprehensive review can be found in [3][35], which we used as the primary references for this section.

5.1 Mathematical models

Mathematical modelling is the earliest method used to formulate epidemic spread [3]. It is mainly characterised by the assumptions of a *homogeneous and well-mixed population* where the epidemic occurs. These simplifications allow the mathematical models to perform a simple analysis of the epidemic diffusion's macroscopic behaviour, such as estimating the epidemic threshold and final epidemic size. At the same time, these assumptions also prevent mathematical models from representing the spread of epidemics in detail, completely *ignoring the fluctuations* of the process and the *heterogeneous nature* of epidemic spreading that is naturally present in the heterogeneous contagiousness of infectious individuals and the heterogeneous connections among them.

5.1.1 Deterministic SIR model

The SIR model is one the most famous *compartmental* epidemic model. The name derives from the fact that these types of models split the population into different "compartments". In the SIR model, these are:

- the S type (Susceptible) are the individuals of the population who have yet to contract the disease and can therefore be infected;
- the I type (Infected) are the individuals of the population carrying the disease and can potentially infect S individuals;
- the R type (Recovered/Removed) are the individuals who do non-participate anymore in the epidemic process because they became immune to the disease or deceased.

Transitions of the agents between different compartments are formulated in the SIR model using this set of ODE [3]:

$$\begin{cases} \frac{ds(t)}{dt} = -\beta s(t) i(t) \\ \frac{di(t)}{dt} = \beta s(t) i(t) - \gamma i(t) \\ \frac{dr(t)}{dt} = \gamma i(t) \end{cases} \tag{5.1.1}$$

here $s(t)$, $i(t)$, and $r(t)$ are the densities of susceptible individuals, infectious in-

Figure 6: Compartmental SIR model with transition rates between states S,I and R.

dividuals, and recovered individuals, respectively. β is called the infection rate; γ is the recovery rate. The temporal evolution of $s(t)$, $i(t)$, and $r(t)$ is described in Fig.(7). For epidemic models, one of the main goals is to find conditions under which a disease introduced into the population will develop into a large outbreak. The key parameter in this regard is the *basic reproductive number*, R_0, defined as the number of secondary infective cases per primary case in a completely susceptible population. In the SIR model to obtain its value, we rewrite equation (5.1.1) as :

$$\frac{di(t)}{dt} = \left(\frac{\beta}{\gamma}s(t) - 1\right)\gamma i(t) \tag{5.1.2}$$

the basic reproduction number is then $R_0 = \frac{\beta}{\gamma}$. When $R_0 > R_{0,c} = 1$, an infectious individual can spread the epidemic across the population. Moreover at the early stage of the epidemics, if we consider the limit $i \simeq 0$ which is approimatelly valid at the ealy stage of the outbreak, we can linearize the previous system of equation obtaining:

$$\frac{di(t)}{dt} \simeq (\beta - \gamma)\, i(t) \tag{5.1.3}$$

whose solution

$$i(t) \simeq i(0)e^{(\beta-\gamma)t} \tag{5.1.4}$$

shows indeed how for $R_0 > 1$ the early time evolution of the number of the infected individuals is exponential. The temporal evolution of infectious individuals with different R_0 is illustrated in Fig(7).

5.1.2 Stochastic SIR model

While deterministic epidemic models are usually described using differential equations as seen above, stochastic epidemic models are typically built using stochastic processes, such as Markov Chains. In the simple case of the SIR model, it is possible to see the connection between these apparently different epidemic modelling ways very clearly. An underlying structure at the basis of the class of stochastic compartmental models is the *Poisson process*. Suppose now to have only one compartment

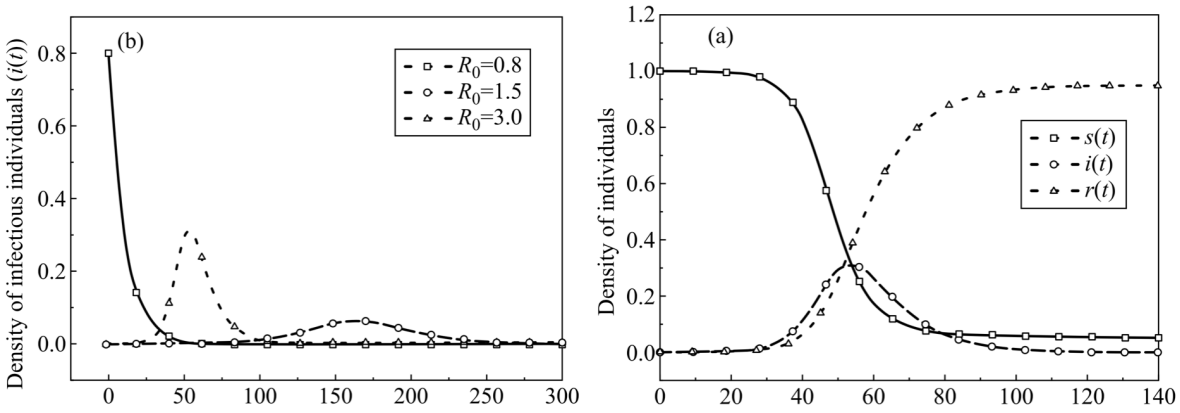

Figure 7: From [3] results of the SIR model (number of individuals $N = 10^4$). (a) Temporal evolution of densities of susceptible, infectious, and recovered individuals ($\beta = 0.3,\ \lambda = 0.1,\ i(0) = 10^{-4}$); (b) temporal evolution of densities of infectious individuals with different basic reproduction number ($R_0 = 0.8 : i(0) = 0.8;\ R_0 = 1.5\ and\ R_0 = 3.0 : i(0) = 10^{-4}$).

in our model with $X(t)$ people already inside at time t and with a simple Poisson process describing the evolution of the number of people inside it. Being the Poisson process a rare event process it is true that:

$$P(X(t + \Delta t) - X(t) = 1) = \lambda \Delta t + o(\Delta t), \tag{5.1.5}$$

where λ is called the stochastic rate of the process. Then the waiting time between two successive increment of the process will be distributed exponentially with parameter λ. However instead of being a constant $\lambda = \lambda(t)$ may depend on time or on the value of the stochastic process at time t as well. If for instance each individual generates another one in the compartment at a stochastic rate a, the total rate of generating another person in the compartment conditioning on the fact that there are already $X(t)$ people inside will be $aX(t)$ thus:

$$P(X(t + \Delta t) - X(t) = 1) = aX(t)\Delta t + o(\Delta t), \tag{5.1.6}$$

This is known as a *pure birth process* and $aX(t)$ is called the conditional instantaneous stochastic rate. Complete now the picture inserting the SIR compartments where S, I and R label the compartments themselves and represent at the same time the numbers of individuals in each compartment. Since the total number of individuals in the population N stays the same during the epidemic, $S + I + R = N$ it is sufficient to consider the process $(S(t), I(t))$ when studying the spread of the disease. If we interpret now β and γ as *probabilistic rates* this time we obtain in the

time interval $[t, t+\Delta t]$:

$$\begin{aligned} &P\left\{[S(t+\Delta t), I(t+\Delta t)] - [S(t), I(t)] = [-1, 1]\right\} = \beta \tfrac{S(t)I(t)}{N}\Delta t + o(\Delta t) \\ &P\left\{[S(t+\Delta t), I(t+\Delta t)] - [S(t), I(t)] = [0, -1]\right\} = \gamma I(t)\Delta t + o(\Delta t). \end{aligned} \tag{5.1.7}$$

This model is known as the general stochastic epidemic [36]. From the previous equations (5.1.7), we can express the increments of S and I in Δt as the sum of the expected value of the increment plus one of a centred increment:

$$\begin{aligned} S(t+\Delta t) - S(t) = \Delta S &= \left(-\beta \tfrac{S(t)}{N}\right)\Delta t + \Delta Z_1 \\ I(t+\Delta t) - I(t) = \Delta I &= \left(\beta \tfrac{S(t)I(t)}{N} - \gamma I(t)\right)\Delta t - \Delta Z_1 + \Delta Z_2 \end{aligned} \tag{5.1.8}$$

where ΔZ_1 and ΔZ_2 are conditionally centered Poisson increments with mean zero and conditional variances $\beta \frac{S_t I t}{N}\Delta t$ and $\gamma I(t)\Delta t$. If we now take the expected value of both quantities, divide by N and let Δt go to zero we see how we obtain the equations (5.1.1). R_0 is defined this time then as the *expected* number of secondary infective cases per primary case in a completely susceptible population. It is clear now how the ODE model can be considered the deterministic skeleton of the corresponding stochastic model, obtained when we ignore the intrinsic fluctuations present in the random evolution of the epidemic. While there are multiple types of stochastic mathematical models other than the simple example we have shown, they are best employed in more elaborate models beyond the mathematical ones that also consider the various heterogeneities present in the spread of an epidemic. Stochastic modelling is also fundamental when the population under study is sufficiently small that is not possible to neglect stochastic fluctuations in the spread of the epidemic. Indeed, As previously stated while an $R_0 > 1$ is a necessary and sufficient condition for the wide spread of the disease in the deterministic model, for a stochastic model is just a necessary condition since stochastic fluctuations can lead to the extinction of the number of infected individuals even for $R > 1$.

5.2 Complex network models

In more complex topologies, epidemic systems are described in complex networks where the vertices represent individuals and the edges the interaction among them. In the compartmental models' framework, the state of each node i at time t is specified by a random variable $X_i \in \{0, 1, \ldots, q-1\}$ where $X_i(t) = \alpha$ indicates that the individual described by node i belongs to the compartment α at time t. As presented before, all the transitions between compartments are described by Poisson process with their rate. However, when the number of individuals in the

network grows too much, it becomes challenging and often useless to keep track of the exact joint probability of the process $P[X_1(t) = x_1, \ldots, X_N(t) = x_N]$ since we are mostly interested in the stationary behaviour of the epidemic or its final size. For this reason, complex network models of epidemics are studied either recurring to numerical simulation or with the aid of mean field theory to recover some analytical understanding. The main mean field approaches as described in [35] are generally:

- **Individual based mean field approach (IBMF):** The idea behind this method is to consider the evolution of $p^{x_i}_{X_i}(t)$, that is the probabilty that node i is in compartment x_i at time t, as statistically independent on the state of its neighbour that is: $P[X_i = x_i, X_j = x_j] = p^{x_i}_{X_i}(t)p^{x_j}_{X_j}(t)$
- **Degree based mean field approach (DBMF):** The DBMF approximation assumes that all the nodes with the same degree k are statistically equivalent, which implies that instead of considering quantities like ϕ_i that specify the state of node i, we work using variables ϕ_k that specify the state of nodes with degree class k. Therefore, instead of working with $p^{x_i}_{X_i}(t)$, in the DBMF approximation we consider $p^{\alpha}_{k}(t)$: the probability that an individual in the population with degree k is in compartment α.

With the aid of mean field theory as shown in [37] a SIS spreading dynamic in an exponential network (Watts-Strogatz or Erdős–Rényi) can be expressed using the following system of equations:

$$\begin{cases} \frac{ds(t)}{dt} = -\lambda\langle k\rangle s(t) + i(t) \\ \frac{di(t)}{dt} = -i(t) + \lambda\langle k\rangle s(t) \end{cases} \tag{5.2.1}$$

where $\lambda = \frac{\beta}{\delta}$, defined as the average infection rate, is composed of: β which measure the probability that a sane individual will get infected if in contact with an infected node and $\delta = 1$ for generality that measure the probability that an infected node will become sane again at the successive time step of the process. These equations, as explained in the network section, are a direct consequence of the democratic feature of exponential networks, where all nodes have a degree k approximately equal to the average value $\langle k\rangle$ in the network. On this type of topology the disease in the network does not become endemic unless $\lambda > \lambda_c = \frac{1}{\langle k\rangle}$. Due to the strong heterogeneity of node degrees however, in scale free network according to DBMF is appropriate to divide nodes in more classes depending on k. Using this approximation the spreading of the epidemic can be described with the following system of equations:

$$\begin{cases} \frac{ds_k(t)}{dt} = -\lambda k s_k(t)\Theta\left(i_k(t)\right) + i_k(t) \\ \frac{di_k(t)}{dt} = -i_k(t) + \lambda k s_k(t)\Theta\left(i_k(t)\right) \end{cases} \tag{5.2.2}$$

where $s_k(t)$ and $i_k(t)$ are the densities of susceptible and infectious nodes with degree k at time t respectively. $\Theta(i_k(t))$ is the probability that any given link connects to an infected node. In the SIS model for this type of networks the epidemic threshold is $\lambda_c = \frac{\langle k \rangle}{\langle k^2 \rangle}$ meaning that if $\langle k^2 \rangle \to \infty$ the epidemic will no matter what reach an endemic state in the network which is a completely different behaviour than the one observed in exponential networks. In the next section we will give details on the epidemiological model we use for the spread of the epidemic in our system.

5.3 SIRD metapopulation model

The Metapopulation network is often used to model (among other phenomena) the global spreading of infectious diseases when the population under study is organised and localised in well defined social units (e.g. families, towns, cities) with some connections among each other [4][21]. The course of an epidemic inside a network was shown to depend significantly on the topology and heterogeneities of the network itself in which it spreads [38][35] as described in the previous sections. Therefore, we decided to choose this metapopulation model, which resembles the most a human structured population [39]. We will now describe the two steps that characterise the metapopulation model of the spreading of the disease. A visual representation of the processes can be found in Fig.(8)

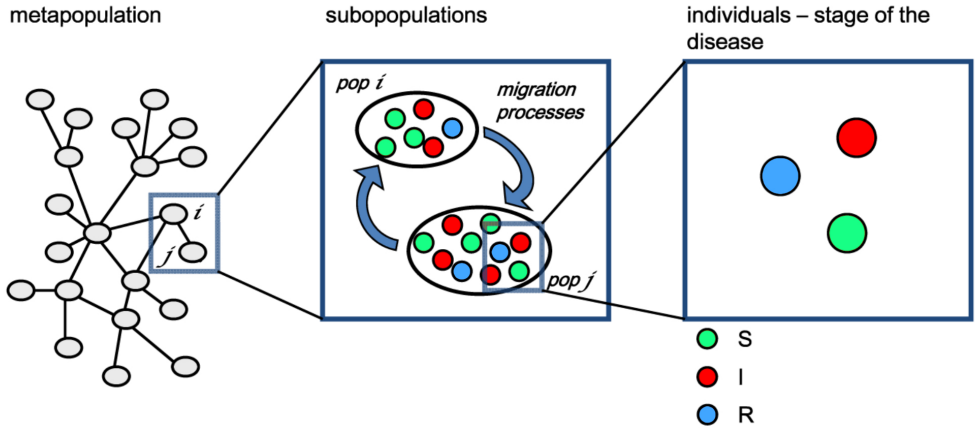

Figure 8: Image from [4]: schematic representation of a metapopulation model with a SIR epidemic process.

5.3.1 Diffusion of agents among the subpopulations

As stated before, the interaction among subpopulations results in individuals moving from one subpopulation to the other, if the two subpopulations are connected. Each subpopulation is characterised by its size $\mathcal{S}_i(t)$: the number of agents who live

there at time t. At the beginning of each time step, every individual can decide to move from their present subpopulation i to a directly connected subpopulation j according to a markovian process characterised by the transition probability matrix d_{ij}. The markovian character of the process is in the fact that we do not label individuals according to their original subpopulation (their hometown). Indeed at each time step, the same diffusion probability applies to all individuals in their current subpopulation without having memory of their origin. As done in [4], we assume that an individual's probability of leaving a given subpopulation is independent of its degree k: $\mu_{k_i} = \mu \ \forall i$ that we will call *diffusion probability*. However given the strong heterogeneity present in the subpopulation network (section 3.3) we do consider heterogeneous diffusion among the subpopulations:

$$\begin{aligned} d_{ij} &= \mu \left[\frac{(k_i k_j)^a}{A} \right] \quad i \neq j \\ d_{ii} &= 1 - \mu. \end{aligned} \tag{5.3.1}$$

Where $\sum_{j \neq i} \frac{(k_i k_j)^a}{A} = 1$. In this way an individual in subpopulation i will move more probably to a bigger and more connected subpopulation, and will move at all from his present subpopulation with probability μ.

5.3.2 Disease diffusion in each subpopulation

After the diffusion step, the disease can spread in each subpopulation. With the aim of simulating the change in the risk propensity of a population in the middle of an epidemic similar to COVID-19 , as several authors did [40][41], we choose a SIRD stochastic model that we tweaked according to our specific needs. The difference between Deceased and Recovered individuals, in fact, is essential in our model since the number of dead nodes in the network is one of the fundamental ingredients that compose the media field in the XY Hamiltonian (section 4.2.3). A schematic view of all the rates and transitions between the different compartments in the model can be found in Fig.(9). We will now describe each process in full detail.

Probability of infection

If a S node i is connected to a I node j inside the subpopulation, the probability of the S node of becoming infected is taken to be:

$$p_{SI} = \beta P_i(\text{Exit}) P_j(\text{Exit}) \tag{5.3.2}$$

β is again the contagion rate intrinsic of the disease, but the overall probability this time also depends on *how much the two individuals are willing to risk* by meeting

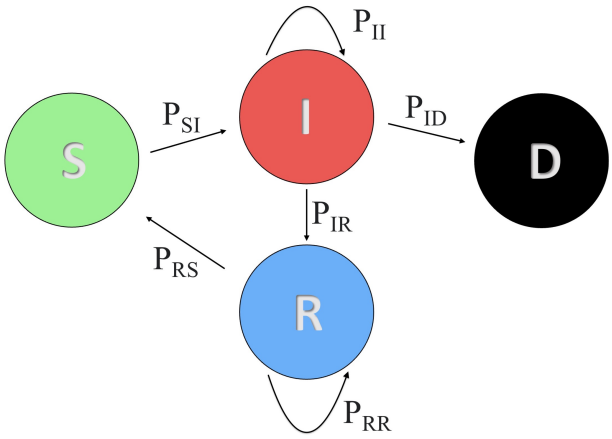

Figure 9: Schematic representation of our modified version of the SIRD model.

other people in the network. Moreover, if an S individual i is connected to several infected nodes, his total probability of contracting the disease will be:

$$p_{SI}^{(\text{tot})} = 1 \quad - \prod_{j \in \partial i : X_j = I} [1 - \beta P_i(\text{Exit}) P_j(\text{Exit})] \tag{5.3.3}$$

After an individual becomes infected, for simplicity, it will remain so for a deterministic time T_I, after which it will become a deceased node or a recovered one. Therefore if node i becomes infected at time t_I:

$$p_{II}(t) = \begin{cases} 1, & t - t_I \leq T_I \\ 0, & t - t_I > T_I, \end{cases} \tag{5.3.4}$$

where p_{II} is the probability that an infected individual remains infected.

Probability of Death and Recovery

If an individual has been infected for T_I time at the next evolution of the SIRD model, he will become a deceased or a Recovered individual. The age distribution in the population is one of the main parameters that drives towards the Zero Risk Society in our model and is a factor that for sure influences the probability that a disease will have an ill-fated course. For this reason, we have modelled the probability of dying because of the disease as:

$$p_{ID}(\Theta) = \sigma(\Theta)\delta \tag{5.3.5}$$

$$\sigma(\Theta) = 1 - \left[1 + \exp\left(\frac{\Theta_c - \Theta}{\mathrm{s}}\right)\right]^{-1} \tag{5.3.6}$$

where the parameter *death probability* δ measure the probability of death of the least healthy individuals in the population while $\sigma(\Theta) \in [0, 1]$, $\sigma(\Theta = 0) = 1$ is a sigmoid function that helps us deciding which age group will be the most hit by the epidemic by tuning the threshold parameter *age lethality* Θ_c, and the probability of having rare events like the death of a very young and healthy individual by tuning the slope parameter s. Since we would like to describe an epidemic similar to COVID19 we fitted this sigmoid curve with the available data of case fatality rates by age in Italy from [42] obtaining (see Fig. 10):

- $\Theta_c = 0.30$;
- $s = 0.05$;
- $\delta = 0.22$.

Probability of rebecoming S

If an individual has become recovered in our model we consider the possibility that he will become susceptible again with a given probability p_{RS}. This models the fact that the immunity acquired by an individual may not last forever. This probability is tuned thanks to the parameter:

$$\begin{aligned} p_{RS} &= \alpha \\ p_{RR} &= 1 - p_{RS}. \end{aligned} \tag{5.3.7}$$

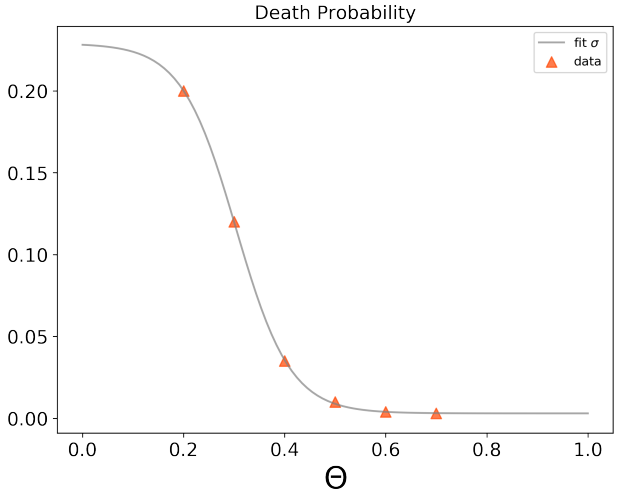

Figure 10: probability of dying after becoming infected

6 Recap

Now that all the elements of the models have been displayed we can give here an overall schematic of the dynamic of our model shown in Fig(11). In the end, briefly, we will also explain the subtle but straightforward connections between this model and the I Zero Risk Society model.

Model parameters

- Health capital distribution $P(\Theta)$ (section 2): a more elder and therefore more settled and susceptible to a disease population will be more risk averse than a younger one;
- Management by extreme Γ (section 4.2.3): measure how much the media relentlessly distorts reality by focusing and amplifying extreme rare events that happens in the population;
- Social media connectivity SMC (section 3.2): tune how much individuals will imitate and will be influenced by their neighbours and popular agents in the network.

In Fig (11), in bold and red we highlighted the term that contribute to advancing towards the zero risk society and our control parameters respectively: the news spread by the media $\{h_{m,i}\}$ together with the management by extremes Γ, the imitation behaviour in the social media network J_{ij} controlled by SMC and the overall influence of the aging of the population described by the health capital distribution Θ. In the picture is clear how the MCMC, governing the spread of information in the social media network, influences the advancing of the epidemic in the network by directly tuning the probability of infection. On the other hand how much the disease is spreading not only will influence directly the individual risk propension of the agents but will also feed the media machine and determine the deceased node. All this contributions amplified by the herding and imitation behaviour, made possible by the social media connections, will strongly influence the final risk propension of each individual $P_i(\text{Exit})$, pushing inevitably to a frozen, paralysed and risk averse society.

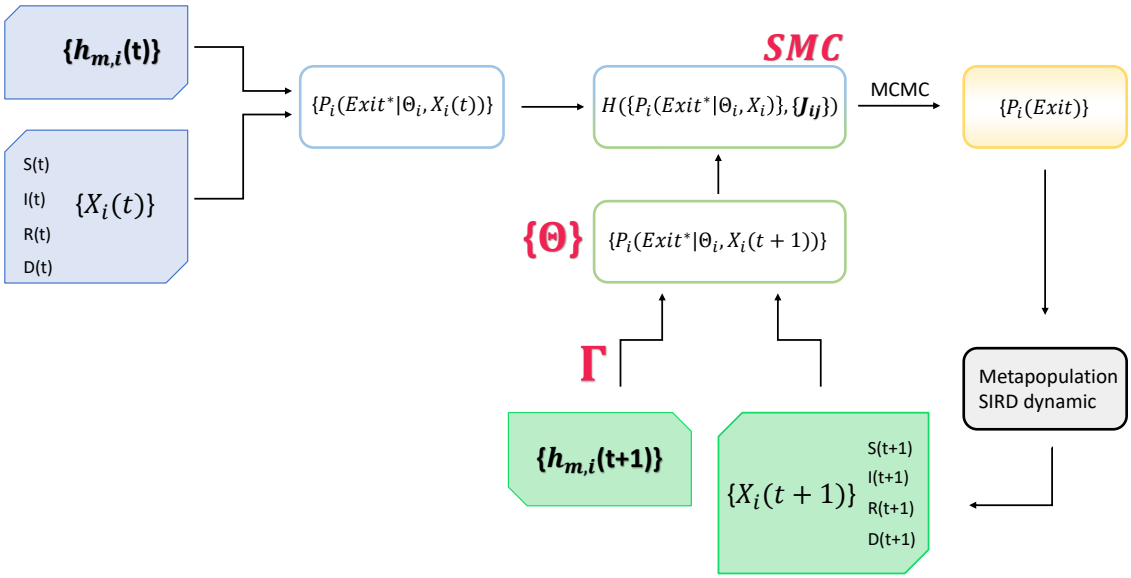

Figure 11: Schematic review of our algorithm for the evolution of people risk propension in the middle of an epidemic.

The I Zero Risk Society: As mentioned in the introduction, in the other project of the Zero Risk Society is not the health of the population at risk but his wealth. As better explained in the original paper [2] and the introduction, in a Zero Risk Society, the population is in a frozen state that concern the lack of investments in innovative researches that may advance humanity rather than a state of fear due to a spread of an epidemic. Indeed the agent i this time will not be puzzled by the decision not to confine himself but rather how much splitting his wealth W_i among a safe asset $r_0 = 0$ and a risky asset $r \in [-1, +\infty]$ so his wealth after the investment will be:

$$W_{t+1} = W_t(1 + (1 - a)r_0 + ar), \tag{6.0.1}$$

a being the percentage of the wealth invested in the risky asset. As in the case of the COVID model, by investing money in the risky asset (that is, by going out), the individual will take the chance of becoming poorer (of becoming infected). Despite this only conceptual difference, however, the structure of the models are the same. The backbone of the COVID model is the two coupled stochastic process occurring on the social media network and the metapopulation network. The first is the MCMC of the XY model that accounts for the exchange of information and peers influence between agents across the network. The second is the SIRD model that shapes the world in which agents live and determines their health condition. In the I Zero Risk society project, the first process remains the same, with the

information exchanged being the percentage of money each agent invested in the risky asset. After having decided the investment (how much going out), the second process follows not the evolution of the individuals' health but the evolution of their wealth. The log of the wealth of each individual will vary in time following a Ornstein–Uhlenbeck (OU) process, therefore the wealth itself will follow:

$$dW(t) = \theta\{\hat{\mu} - \mathrm{Ln}[W(t)]\}W(t)dt + \hat{\sigma}W(t)dX(t) \tag{6.0.2}$$

where the drift term can be interpreted as the influence of the welfare state in which individuals live that, loosely speaking, prevents extreme fluctuation of the wealth by taxing extreme wins and by giving aids in case of extreme losses . The Noise term dX account for the volatility of the investment. Some agents will be lucky and will see their wealth increase; others will not and will experience a wealth loss $\Delta W_i < 0$. The media then, cunningly selecting the agents who experienced the worse losses by an amount tuned by the same management by extremes parameter, will spread a risk-averse idea across the network. As in the COVID model then, older and wealthier people tend still to be more risk averse towards investing in a very risky asset being more interested in preserving their present wealth; so in this model the age and,in particular, the initial wealth distribution of the population will play a crucial role in determining the risk propensity of the population. Finally, as stated in the Introduction, the I Zero Risk Society model account also for the people who cannot afford to invest any of their money in the asset because of living in extreme poverty conditions and not having access to this opportunity. In the I Zero Risk Society model, the probability of an agent of not being able to invest is given by a sigmoid function $\sigma(W)$ and these agents will be represented by spins pointing in the y direction. These agents and the mechanism by which they are selected are comparable to the deceased node in the COVID model. More information on this model can be found on the thesis of my colleague and friend Giuseppe Aventaggiato. Table 1 summarise the similarities between these to model.

I Zero Risk	**COVID model**
$P(W)$ wealth distribution in the population	$P(A)$ age distribution in the population
$(\mathbf{s}_i)_x = \sqrt{a}$	$(\mathbf{s}_i)_x = cos(\theta)$
$(\mathbf{h}_i)_x = W_i\sqrt{a^*}$	$(\mathbf{h}_i)_x = \Theta_i k_i cos(\theta^*)$
$J_{ij} = W_i \| W_j$	$J_{ij} = (\Theta_i\Theta_j) \| (k_i k_j)$
media $v(t) = \sum_{i=1}^{\Gamma} \frac{\lvert\Delta W_i\rvert}{\Gamma},\ \lvert\Delta W_i\rvert > \lvert\Delta W_{i+1}\rvert$	media $v(t) = \sum_{i=1}^{\Gamma} \frac{\Theta_i^x}{\Gamma},\ \Theta_i^x > \Theta_{i+1}^x$
OU process for wealth evolution	SIRD model for healths evolution
MCMC for information on the investiment	MCMC for information on the confinement
No acces to opportunity	Deceased nodes

Table 1: I Zero Risk Society and COVID model confronted.

7 Results

In this section, we show the results we obtained so far with our preliminary simulations aimed at exploring the parameters space of our model. The simulations have been done considering $N = 625$ agents spread across 15 subpopulation with an average number of 40 individuals each at the beginning. Each simulation consisted in 600 macro-steps of the model. Each macro-step consist in the thermalizaton of the XY model using the MCMC and one evolution of the SIRD epidemic. The temperature in the MCMC evolution has been set to 0 in all the simulations for the sake of simplicity. In Figs.(12,13) we show a snapshot of the XY process and of the SIRD process.

7.1 Disease parameters

In all the simulations we made, we set the disease parameter as the following:

- diffusion probability: $\mu = 0.9$;
- contagion rate: $\beta = 0.9$;
- infection time: $T_I = 4$;
- death probability: $\delta = 0.22$;
- age lethality: $\Theta_c = 0.3$;
- return to susceptibility: $\alpha = 0.5$.

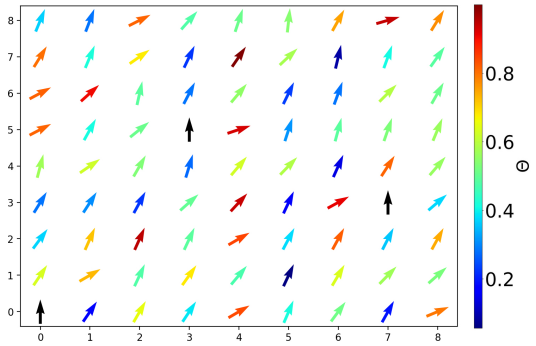

Figure 12: Snapshot of the XY model during the spread of informations. We can clearly see how younger spins lay flatter along the x axis (i.e. they are more risk inclined). Black spins pointed in the y direction represent deceased individual.

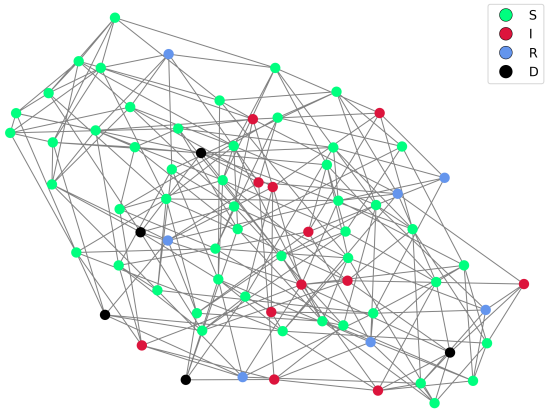

Figure 13: Snapshot of a subpopulation during the spread of the epidemic.

The disease parameter we set, except for the death probability as presented in the previous section, are quite unrealistic and tuned for having a wide and fast spreading of the epidemic across the network. This was necessary at this stage since usually epidemic and metapopulations models are analysed with $\sim 10^3$ subpopulations with, on average, 10^3 individuals each, for a total of $\sim 10^6$ agents. In Figs.(14,15), we can see the evolution of the SIRD dynamic and the individual risk propension averaged over multiple random number generator seeds. In Fig.(16) instead we can appreciate the value $V(t)$ of the media field when varying Γ. As presented in the section (4.2.3) we can see how a little Γ in the same simulation with the other control parameters fixed, and therefore with the same objective news that can be reported, results in a more aggressive media with a modulus comparable to the field modulus of the younger share of the population.

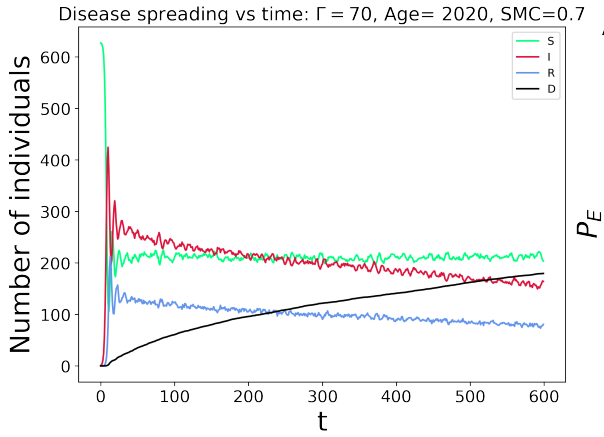

Figure 14: Evolution of S,I,R,D individuals in time, averaged over several seeds. $S(0) = N - 1, I(0) = 1$.The age distribution is the one of the world in 2020.

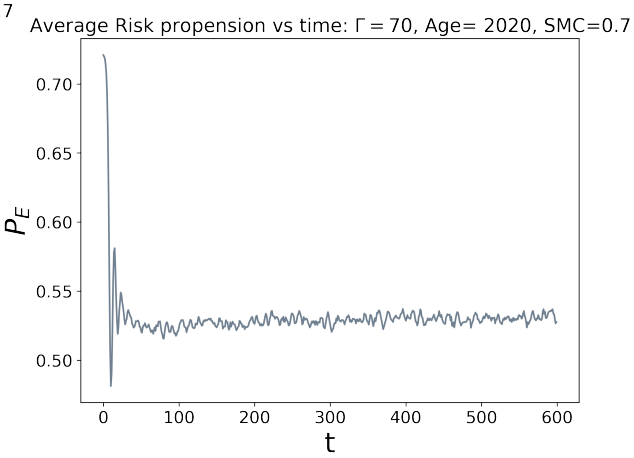

Figure 15: Evolution of the average risk propension in the population in time, averaged over several seeds.The age distribution is the one of the world in 2020.

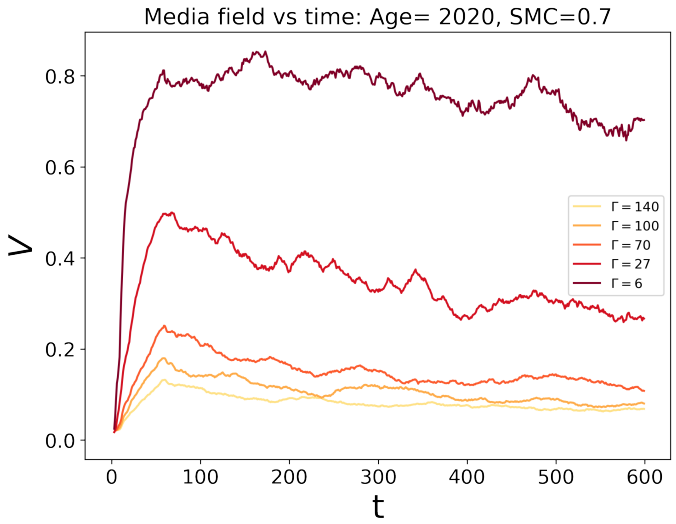

Figure 16: Evolution of the value of V in time, averaged over several seed of the random number generator and for different value of Γ.

7.2 Model Parameters

Despite the small scale of the simulations, the results we obtained so far by varying the control parameters of the model are promising and align well with our intuitions. In Fig.(17) we can observe how the influence of a more and more aggressive media that distorts the facts and focuses on the worst possible events in the community leads to a decreasing risk propension of the population. The simulation points were fitted using the function:

$$f(x) = ax^c + b, \tag{7.2.1}$$

obtaining:

- $a = 2.74 \cdot 10^{-2}$, $b = 4.70 \cdot 10^{-1}$, $c = 2.25 \cdot 10^{-1}$ for age w 1950;
- $a = 2.48 \cdot 10^{-2}$, $b = 4.60 \cdot 10^{-1}$, $c = 2.33 \cdot 10^{-1}$ for age w 2020;
- $a = 1.40 \cdot 10^{-2}$, $b = 4.47 \cdot 10^{-1}$, $c = 2.81 \cdot 10^{-1}$ for age ITA 2040.

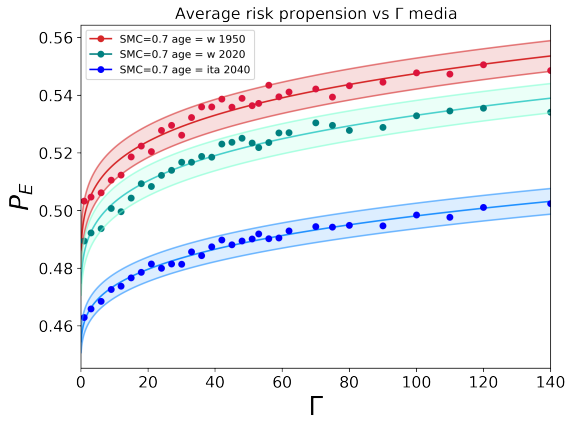

Figure 17: Evolution of the average risk propension in the population vs the value of Γ for different value of the age distribution: world 1950, world 2020 and Italy 2040 forecast. The points showed in the graph, and fitted with EQ. (7.2.1), were averaged over multiple seed of the random number generator.The shaded region was built by fitting EQ. (7.2.1) on the points $P_E(\Gamma) \pm 3\sigma(\Gamma)$, $\sigma(\Gamma)$ being the standard deviation of point $P_E(\Gamma)$.

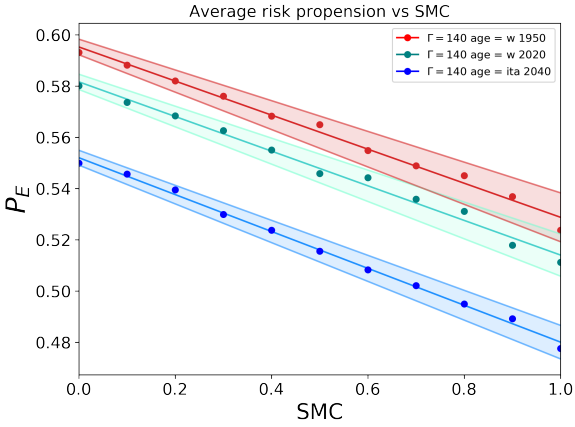

Figure 18: Evolution of the average risk propension in the population vs the value of SMC for different value of the age distribution: world 1950, world 2020 and Italy 2040 forecast. The points shown in the graph, and fitted with EQ. (7.2.2), were averaged over multiple seed of the random number generator. The shaded region was built by fitting EQ. (7.2.2) on the points $P_E(SMC) \pm 3\sigma(SMC)$, $\sigma(SMC)$ being the standard deviation of point $P_E(SMC)$.

Fig.(18), on the other hand, shows the effect of the imitation behaviour in our model and, in particular, how a more connected population with individuals more inclined at imitating each other tends at amplifying the collective risk aversion of the whole system. The simulation points were fitted this time using the function:

$$g(x) = \bar{a}x + \bar{b}, \tag{7.2.2}$$

obtaining this time:

- $\bar{a} = -6.64 \cdot 10^{-2}$, $\bar{b} = 5.95 \cdot 10^{-1}$, for age w 1950;
- $\bar{a} = -6.76 \cdot 10^{-2}$, $\bar{b} = 5.81 \cdot 10^{-1}$ for age w 2020;
- $\bar{a} = -7.20 \cdot 10^{-2}$, $\bar{b} = 5.52 \cdot 10^{-1}$ for age ITA 2040.

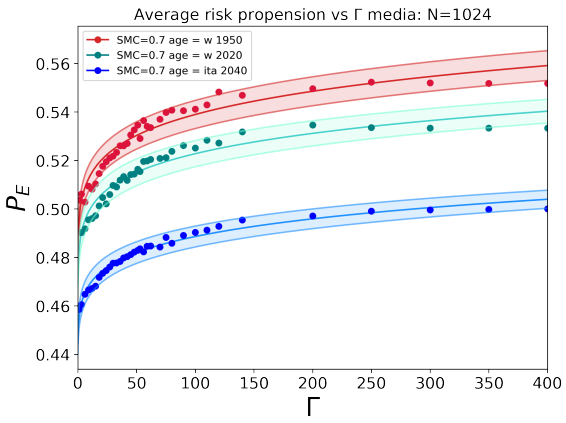

Figure 19: Evolution of the average risk propension in the population $N = 1024$ vs the value of Γ for different value of the age distribution: world 1950, world 2020 and Italy 2040 forecast.

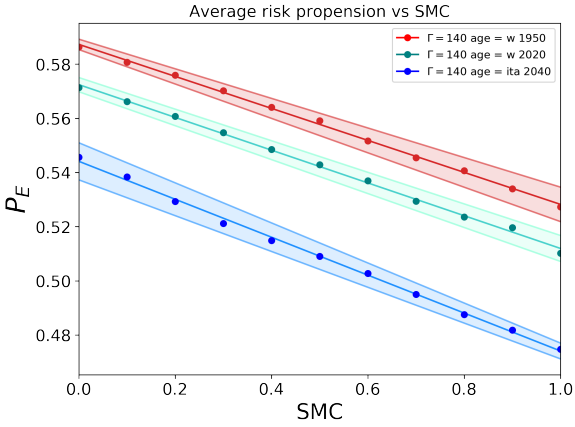

Figure 20: Evolution of the average risk propension in the population $N = 1024$ vs the value of SMC for different value of the age distribution: world 1950, world 2020 and Italy 2040 forecast.

These results are confirmed also for simulations done considering $N = 1024$ and the same number of macro-steps. In particular in Fig(19) it is possible to see a good agreement with the function f also for greater value of Γ. Indeed, the flattening of the simulation points for the greatest values of Γ can be reconduced to the media completely switching from the news about deceased nodes to the news regarding infected ones, artifact that can be eliminated performing simulations with still more agents. A good agreement with function g is obtained as well as it is possible to see in Fig(20). Moreover in both Figs(19,20) is also possible to see how the increased number of agents in the simulation lowered slightly the results obtained for

P_E when compared with Figs(17,18) further confirming how the herding and imitation behaviour is a fundamental contribution in lowering the risk propensity in the system that may have a much greater effect in more scaled up simulation.
Finally, in Fig.(21), we simulated a sweep towards history by simultaneously varying all the control parameters in our model: age distribution, social media connectivity and management by extremes, to mimic the advancement towards a more modernised society. Though the value of these parameters has been assigned qualitatively, we can see how these elements' collective action leads to a non linear decrease in the population's risk propensity when perturbed by a threatening epidemic outbreak. Moreover, this reduction is even stronger in a geriatric population like the one predicted for Italy in 2040.

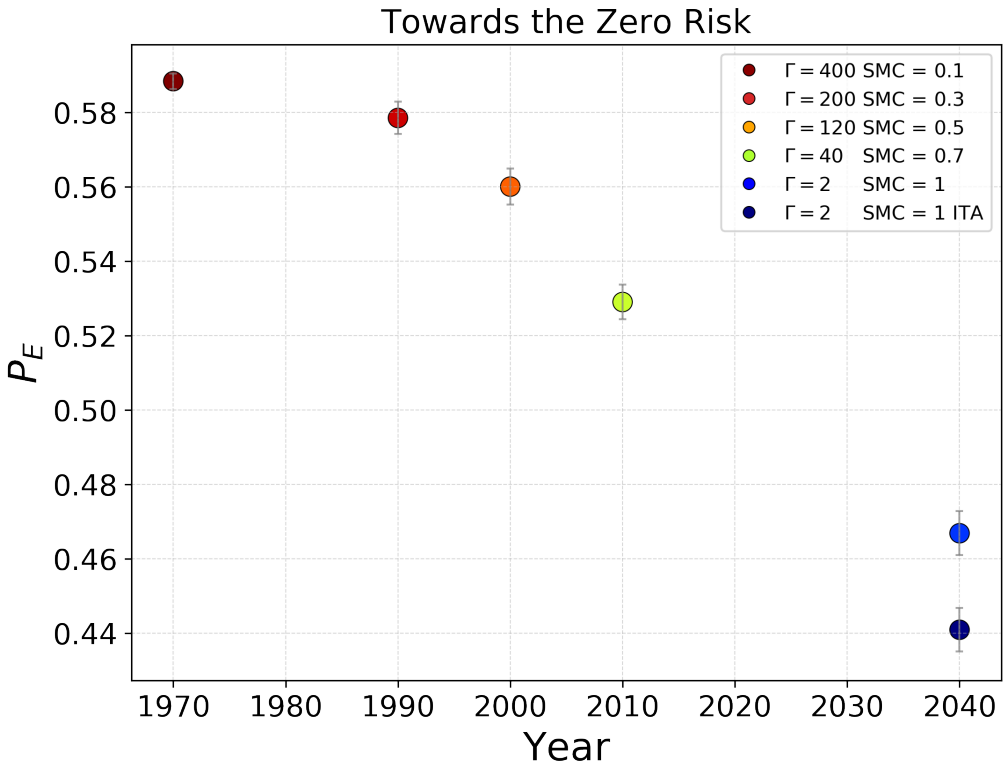

Figure 21: Evolution of the average risk propension in the population obtained by simultaneously varying all the control parameters in our model: age distribution, Γ and SMC, in order to mimic the historical evolution of human society. All the points shown were obtained by averaging over multiple seed of the random number generator. The error bars represent $P_E(i) \pm 3\sigma_i$, where σ_i represent the standard deviation of point $P_E(i)$.

Conclusions

The results we have shown so far show how the elements we identified that lead towards the Zero Risk Society are indeed correct. The same is valid on the I Zero Risk Society project, demonstrating how the ingredients mentioned in the introduction are general and lead to a reduction in the risk propensity of agents independently of the type of "volatility" and perturbation experienced by individuals (fluctuation of wealth or health). Indeed, the simulations showed how the simple model we developed is suitable and results stable for describing the behaviour of a society affected by an external perturbation and with the characterised described in the introduction by finely intertwining all the elements presented so far. No evidence of a phase transition is found at this early stage. However, the model's parameter space has yet to be explored in depth, using more realistic and scaled up simulations. This model however can be used as a first solid brick towards the built of more accurate and refined simulations and models. For example the metapopulation model also allows for several enhancements. In the metapopulation model the "cities" can, for example, be interpreted instead as the home of a small group of individuals, like a family's house. In this way, the probability of being infected may be tweaked, so an individual's choice to naturally stay home during the spread of the epidemic will be counterproductive if there is an infected relative at home. These unexpected transmissions caused by the agents who believe that are behaving correctly may lead to a positive feedback loop where the more the individuals are pushed towards not risking and staying home, the more the pandemic can spread and so forth. The same is true if we symmetries the Hamiltonian by considering a media field that on average point to $\theta_m = \frac{\pi}{4}\ rad$ and study the behavior of P_E around it: $\theta_m = \frac{\pi}{4} + \delta$ that can be interpreted as the media trying to push also a more optimistic agenda so that the subsequent distortion of the facts can have a greater impact on the network.

Personally, I am very satisfied with the result of the model at this stage, given that it was built from scratch by me and my colleague Aventaggiato that shares as much credit as I do for the creation and the results produced by this model, and with whom I was able to share the satisfaction of seeing the first expected results coming out.

References

[1] M. Marsili. Spiraling toward market completeness and financial instability. *Technical report, The Abdus Salam International Centre for Theoretical Physics*, 2009.

[2] Didier Sornette and Peter Cauwels. Trapped in the "zero-risk" society and how to break free (1st sept. 2020) swiss finance institute research paper no. 20-78, available at ssrn: https://ssrn.com/abstract=3684550 published in german as "gefandan in der null risiko-gesellschaft" (caught in the zero-risk society), twice, herbst 2020, pp. 4-7.

[3] Wei Duan, Zongchen Fan, Peng Zhang, Gang Guo, and Xiaogang Qiu. Mathematical and computational approaches to epidemic modeling: a comprehensive review. *Frontiers of Computer Science*, 9(5):806–826, Oct 2015.

[4] Vittoria Colizza and Alessandro Vespignani. Epidemic modeling in metapopulation systems with heterogeneous coupling pattern: Theory and simulations. *Journal of Theoretical Biology*, Volume 251(3):450–467, Apr 2008.

[5] Shannon Fast, Marta C. Gonzalez, James Wilson, and Natasha Markuzon. Modelling the propagation of social response during a disease outbreak. *Journal of the Royal Society, Interface / the Royal Society*, Volume 12, 03 2015.

[6] Paulo Cesar Ventura da Silva, Fátima Velásquez-Rojas, Colm Connaughton, Federico Vazquez, Yamir Moreno, and Francisco A. Rodrigues. Epidemic spreading with awareness and different timescales in multiplex networks. *Phys. Rev. E*, 100:032313, Sep 2019.

[7] populationpyramid.net.

[8] Vito Latora, Vincenzo Nicosia, and Giovanni Russo. *Complex networks: principles, methods and applications.* Cambridge University Press, 2017.

[9] Albert-László Barabási and Réka Albert. Emergence of scaling in random networks. *Science*, 286(5439):509–512, 1999.

[10] P Erdös and A Rényi. On random graphs i. *Publicationes Mathematicae Debrecen*, 6:290–297, 1959.

[11] Duncan J. Watts and Steven H. Strogatz. Collective dynamics of 'small-world' networks. *Nature*, 393(6684):440–442, Jun 1998.

[12] P. Erdös and A. Rényi. On the evolution of random graphs. *Publications of the Mathematical Institute of the Hungarian Academy of Sciences*, 1960.

[13] Réka Albert and Albert-László Barabási. Statistical mechanics of complex networks. *Rev. Mod. Phys.*, 74:47–97, Jan 2002.

[14] A.L Barabási, H Jeong, Z Néda, E Ravasz, A Schubert, and T Vicsek. Evolution of the social network of scientific collaborations. *Physica A: Statistical Mechanics and its Applications*, 311(3):590–614, Aug 2002.

[15] Albert-Laszlo Barabasi and Eric Bonabeau. Scale-free networks. *Scientific American*, May 2003.

[16] G Bianconi and A.-L Barabási. Competition and multiscaling in evolving networks. *Europhysics Letters (EPL)*, 54(4):436–442, may 2001.

[17] Didier Sornette. Dragon-kings, black swans and the prediction of crises. *International Journal of Terraspace Science and Engineering*, 2(1):1–18, 2009.

[18] Ginestra Bianconi and Albert-László Barabási. Bose-einstein condensation in complex networks. *Phys. Rev. Lett.*, 86:5632–5635, Jun 2001.

[19] V. I. Yukalov and D. Sornette. Statistical outliers and dragon-kings as bose-condensed droplets. *The European Physical Journal Special Topics*, 205(1):53–64, May 2012.

[20] Sandro Claudio Lera, Alex Pentland, and Didier Sornette. Prediction and prevention of disproportionally dominant agents in complex networks. *Proceedings of the National Academy of Sciences*, 117(44):27090–27095, 2020.

[21] Jessica T. Davis, Nicola Perra, Qian Zhang, Yamir Moreno, and Alessandro Vespignani. Phase transitions in information spreading on structured populations. *Nature Physics*, Volume 16(5):590–596, Mar 2020.

[22] Haoxiang Xia, Huili Wang, and Zhaoguo Xuan. Opinion dynamics: A multidisciplinary review and perspective on future research. *International Journal of Knowledge and Systems Science*, 2:72–91, 10 2011.

[23] Quanbo Zha, Gang Kou, Hengjie Zhang, Haiming Liang, Xia Chen, Cong-Cong Li, and Yucheng Dong. Opinion dynamics in finance and business: a literature review and research opportunities. *Financial Innovation*, 6(1):44, Jan 2021.

[24] M. J. de Oliveira. Isotropic majority-vote model on a square lattice. *Journal of Statistical Physics*, 66(1):273–281, Jan 1992.

[25] André L. M. Vilela and H. Eugene Stanley. Effect of strong opinions on the dynamics of the majority-vote model. *Scientific Reports*, 8(1):8709, Jun 2018.

[26] G. Grinstein, C. Jayaprakash, and Yu He. Statistical mechanics of probabilistic cellular automata. *Phys. Rev. Lett.*, 55:2527–2530, Dec 1985.

[27] Juan Carlos González-Avella, Mario G. Cosenza, Konstantin Klemm, Víctor M. Eguíluz, and Maxi San Miguel. Information feedback and mass media effects in cultural dynamics. *Journal of Artificial Societies and Social Simulation*, 10(3):9, Jun 2007.

[28] Jozef Strecka and Michal Jascur. A brief account of the ising and ising-like models: Mean-field, effective-field and exact results. *acta physica slovaca*, Volume 65 No. 4, Aug 2015.

[29] Georges Harras, Claudio J. Tessone, and Didier Sornette. Noise-induced volatility of collective dynamics. *Phys. Rev. E*, 85:011150, Jan 2012.

[30] Yusuf Yüksel, Erol Vatansever, Ümit Akınc ı, and Hamza Polat. Nonequilibrium phase transitions and stationary-state solutions of a three-dimensional random-field ising model under a time-dependent periodic external field. *Phys. Rev. E*, 85:051123, May 2012.

[31] Muktish Acharyya. Nonequilibrium phase transition in the kinetic ising model: Dynamical symmetry breaking by randomly varying magnetic field. *Phys. Rev. E*, 58:174–178, Jul 1998.

[32] Peter Vasterman, C. Joris Yzermans, and Anja J. E. Dirkzwager. The Role of the Media and Media Hypes in the Aftermath of Disasters. *Epidemiologic Reviews*, 27(1):107–114, Jul 2005.

[33] Augustine Pang. Social media hype in times of crises: Nature, characteristics and impact on organizations. *Asia Pacific Media Educator*, 23(2):309–336, 2013.

[34] Stuart Soroka, Patrick Fournier, and Lilach Nir. Cross-national evidence of a negativity bias in psychophysiological reactions to news. *Proceedings of the National Academy of Sciences*, 116(38):18888–18892, 2019.

[35] Romualdo Pastor-Satorras, Claudio Castellano, Piet Van Mieghem, and Alessandro Vespignani. Epidemic processes in complex networks. *Rev. Mod. Phys.*, 87:925–979, Aug 2015.

[36] Priscilla E. Greenwood and Luis F. Gordillo. Stochastic epidemic modeling. In Gerardo Chowell, James M. Hyman, Luís M. A. Bettencourt, and Carlos Castillo-Chavez, editors, *Mathematical and Statistical Estimation Approaches in Epidemiology*, pages 31–52. Springer Netherlands, Dordrecht, 2009.

[37] Romualdo Pastor-Satorras and Alessandro Vespignani. Epidemic dynamics and endemic states in complex networks. *Phys. Rev. E*, 63:066117, May 2001.

[38] Romualdo Pastor-Satorras and Alessandro Vespignani. Epidemic spreading in scale-free networks. *Phys. Rev. Lett.*, 86:3200–3203, Apr 2001.

[39] Gerardo Chowell, James Hyman, Stephen Eubank, and Carlos Castillo-Chávez. Scaling laws for the movement of people between locations in a large city. *Physical Review E*, 68, Dec 2003.

[40] Jesús Fernández-Villaverde and Charles I Jones. Estimating and simulating a sird model of covid-19 for many countries, states, and cities. *National Bureau of Economic Research*, (number 27128), May 2020.

[41] Giuseppe C. Calafiore, Carlo Novara, and Corrado Possieri. A time-varying sird model for the covid-19 contagion in italy. *Annual Reviews in Control*, 50:361–372, 2020.

[42] Esteban Ortiz-Ospina Max Roser, Hannah Ritchie and Joe Hasell. Coronavirus pandemic (covid-19). *Our World in Data*, 2020. https://ourworldindata.org/coronavirus.